



Tautomeric equilibrium in trifluoroacetaldehyde arylhydrazones[☆]



Agata Wojciechowska^a, Marcin Jasiński^{a,*}, Piotr Kaszyński^{a,b}

^a Department of Organic and Applied Chemistry, University of Łódź, Tamka 12, 91-403 Łódź, Poland

^b Organic Materials Research Group, Department of Chemistry, Vanderbilt University, Nashville, TN 37235, United States

ARTICLE INFO

Article history:

Received 24 December 2014

Received in revised form 16 February 2015

Accepted 3 March 2015

Available online 7 March 2015

Keywords:

Fluoral

Azo-hydrazone tautomerism

Synthesis

DFT calculations

Correlation analysis

ABSTRACT

A series of *p*-substituted phenylhydrazones of trifluoroacetaldehyde (**1**) was synthesized and the azo-hydrazone (**1–2**) tautomeric equilibrium was investigated experimentally using correlation analysis and computationally with DFT methods. Investigation revealed strong impact of the substituent and solvent polarity on the tautomeric ratio (**1/2**). Calculations also revealed that acidity of the azo tautomers is similar to that of malonate esters.

© 2015 Elsevier Ltd. All rights reserved.

1. Introduction

Tautomeric equilibria in the RCH–X=Y system involving 1,3 proton transfer have been thoroughly investigated in, e.g., carbonyl compounds (keto–enol equilibrium, **Ia–IIa**, X=CR', Y=O, Fig. 1) and for nitroso derivatives (**Ib–IIb**, X=N, Y=O).^{1,2} In contrast, the analogous tautomerism of hydrazones is far less well known in the literature.³ Although examples of complete tautomerization of several azo **Ic** to hydrazone **IIc** derivatives (R=alkyl, R'=aryl, alkyl)^{3e,g} and base-induced tautomerization of hydrazone **IIc** to azo **Ic** (R=alkyl, R'=Ph)^{3d} have been reported, to the best of our knowledge no equilibrating azo-hydrazone tautomeric systems of type **Ic–IIc** have been studied in detail thus far.⁴ Here we investigate such an equilibrium for a series of fluoral derivatives (R=CF₃).

The trifluoromethyl group attracts considerable attention in the context of the preparation of biologically active compounds⁵ and other materials, such as liquid crystals.⁶ In a series of papers, several

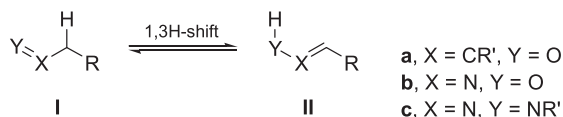


Fig. 1. Tautomeric equilibria **I–II** for carbonyl (**a**), nitroso (**b**), and azo (**c**) compounds.

hydrazones of type **IIc** (R=CF₃) were demonstrated as superior building blocks for the construction of N-heterocyclic systems, mainly pyrazole and pyridazine derivatives,⁷ including compounds of biological importance.^{7d} The report by the Rueping group on enantioselective synthesis of trifluoromethylated 1,4-dihydropyridazines is especially worth mentioning.^{7h} Interestingly, the key step in this reaction is apparently C-nucleophilic attack of the hydrazone **IIc** (R=CF₃) facilitated by increased importance the 1,3-dipolar resonance form (Fig. 2).^{7h}



Fig. 2. Two resonance forms of trifluoroacetaldehyde hydrazones.

The azo tautomers **Ic** (R=CF₃) have not been described in the literature, although they could also be useful in construction of trifluoromethylated pyridazines through a hetero-Diels–Alder reaction, as has been demonstrated for some other arylazoalkanes.⁸

Recently, we also used hydrazones **IIc** (R=CF₃) to introduce the CF₃ group as a polar substituent in liquid crystalline derivatives of verdazyl.⁹ We observed that one of the intermediates, hydrazone **1a**, exists in equilibrium with its azo form **2a** (Fig. 3). We speculated, that the position of the equilibrium should correlate with electron density in the π system modulated by a substituent on the phenyl ring, and also reflect on the nucleophilic nature of the C atom in hydrazones **1**. Therefore, a series of trifluoroacetaldehyde *p*-substituted phenylhydrazones, **1a–1k** were synthesized and

[☆] Part of the MSc thesis of A.W., University of Łódź, 2014.

* Corresponding author. Tel.: +48 42 635 57 66; fax: +48 42 665 51 62; e-mail addresses: mjasinski@uni.lodz.pl (M. Jasiński), piotr.kaszyński@vanderbilt.edu (P. Kaszyński).

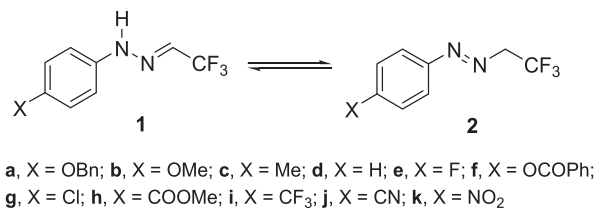
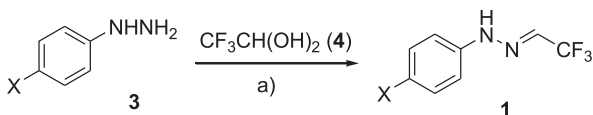


Fig. 3. Azo-hydrazone tautomeric equilibrium 1–2 for fluoral derivatives.

investigated in detail in the context of tautomeric equilibrium with the corresponding azo form **2** (Fig. 3). Here we demonstrate experimental and computational results of the substituent and solvent effects on the equilibrium position in the tautomeric pairs 1–2, and provide more insight into synthetic applications of the hydrazones.

2. Results and discussion

p-Substituted phenylhydrazones **1a–1k** were obtained in the pure form in 38–94% yield according to a general procedure¹⁰ by heating methanolic solutions of the appropriate hydrazine **3** and fluoral hydrate (**4**) in a closed ampoule at 75 °C overnight, in the presence of molecular sieves 4 Å (Scheme 1). The lowest yield was obtained for the hydrazone bearing the methoxycarbonyl substituent (**1h**) due to its limited stability in solutions and solid state.



Scheme 1. Synthesis of hydrazones **1**. Reaction conditions: (a) MeOH, mol sieves 4 Å, closed ampoule, 75 °C, 16 h.

Initial experiments were conducted with 4-benzyloxy hydrazone **1a**. Its attempted purification by column chromatography on silica gel failed, and only the corresponding azo derivative **2a** was obtained in 30% yield, presumably as a result of acid-catalyzed isomerization accompanied by partial hydrolysis of the hydrazone **1a**. Derivative **2a** is the only azo compound in the series that was isolated in the pure form.

The ¹H NMR spectrum of a freshly recrystallized sample of **1a**, taken in CDCl₃, showed a single set of signals indicating the presence of the pure hydrazone. The diagnostic signal attributed to the azomethine hydrogen (=CHCF₃) was found at 6.91 (qd, *J*_{H–H}=1.4 Hz, *J*_{H–F}=4.1 Hz) ppm. After 30 min the ¹H NMR spectrum showed the appearance of a new single set of signals attributed to the *trans*-azo tautomer **2a** with the characteristic signals of the CH₂CF₃ group at 4.43 (q, *J*_{H–F}=9.7 Hz) ppm. Further monitoring of the sample showed, that after 10 h the mixture of **1a–2a** equilibrated at 27:73 ratio (Fig. 4). Kinetic analysis of the data indicates a first-order process with a rate of *k*=1.79(6)×10^{−3} min^{−1}. Similarly, pure **2a** dissolved in CDCl₃ gave the same ratio of tautomers within a few hours.

The isolation of pure **1a** and **2a** permitted analysis of electronic absorption spectra for the individual tautomers, which were recorded in MeCN and are shown in Fig. 5. Both compounds showed single strong absorption band with a maximum at about 290 nm, and with a shoulder absorption at about 320 nm. In addition, the orange azo tautomer **2a** exhibits two weak overlapping absorption bands at about 400 and 500 nm.

Interestingly, exposure of the NMR tube containing the equilibrium mixture of **1a** and **2a** to sunlight for 2 h shifted the equilibrium to a nearly equimolar ratio of the tautomers (52:48). Longer exposure to sunlight showed no further changes in the ratio, while

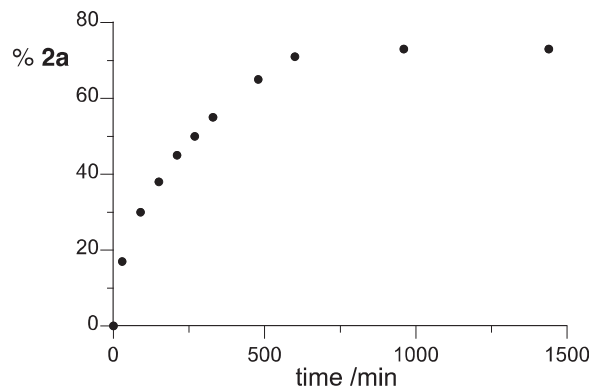


Fig. 4. Formation of azo **2a** in a CDCl₃ solution at ambient temperature by tautomerization of the hydrazone form **1a**.

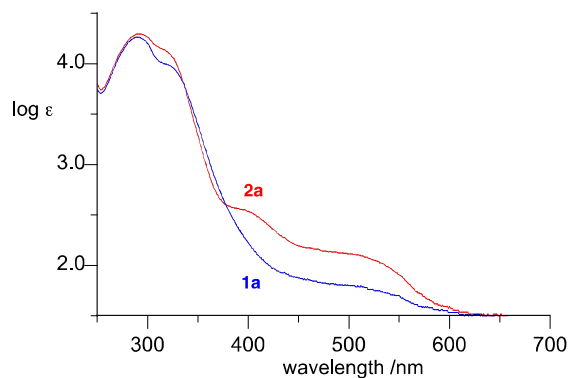


Fig. 5. Electronic absorption spectra for **1a** (blue) and **2a** (red) in CH₃CN.

storing the sample in the dark overnight shifted the equilibrium back to the original tautomeric equilibrium of **1a–2a**. No such photo-induced changes were observed for **1c** in CDCl₃.

¹H NMR spectra of other hydrazones, **1b–1f**, also showed the formation of the respective tautomeric azo forms **2b–2f**, with the equilibrium points reached typically within 8–14 h in CDCl₃. However, in the case of derivatives containing strongly electron-withdrawing groups, COOMe (**1h**), CF₃ (**1i**), CN (**1j**), and NO₂ (**1k**), only trace amounts of the corresponding azo derivatives (<3%) were observed. Pure azo tautomers **2b–2f** could not be isolated and they were investigated as mixtures with the hydrazone forms.

As in the case of **1a–2a**, the ratio of the tautomers *K* (Table 1) was typically established using the characteristic signals in the ¹H NMR spectra attributed to the azomethine (6.90–7.13 ppm range) and methylene hydrogen atoms (4.43–4.56 ppm range). Similar

Table 1
Experimental and theoretical equilibrium constant *K* for tautomers **1** and **2**

	R	<i>K</i> _{exp} ^a	<i>K</i> _{theor} ^b	σ _p ^c
a	OBn	0.4	—	— ^d
b	OMe	0.3	2.1	−0.27
c	Me	1.8	29.2	−0.17
d	H	6.1	64.9	0.00
e	F	2.0	16.9	0.06
f	PhCOO	4.0	—	0.13
g	Cl	6.7	390	0.23
h	COOMe	49 ^e	3250	0.45
i	CF ₃	99	3130	0.54
j	CN	199	8734	0.66
k	NO ₂	~10 ³	33,990	0.78

^a Equilibrium after 5 d (rt, in dark) in CDCl₃ solution.

^b M062X/6-31G(2d,p) calculations in the CDCl₃ medium.

^c Ref. 11.

^d Not known.

^e Partial decomposition of **1h** and **2h** in CDCl₃ solution.

diagnostic chemical shifts were found in the ^{13}C NMR spectra of the series: signals attributed to $\text{N}=\text{CH}-\text{CF}_3$ atom were located in the range 121.3–122.7 ($^2J_{\text{C}-\text{F}}=39$ Hz) ppm, whereas signals of the $\text{N}-\text{CH}_2-\text{CF}_3$ carbon atom were found in the region 68.5–68.8 ($^2J_{\text{C}-\text{F}}=29$ Hz) ppm.

In general, increasing the electron-withdrawing character of the substituent X decreases shielding of the diagnostic ^1H and ^{13}C nuclei in both series of compounds, hydrazones **1** and azo **2** (Fig. 6). In contrast, ^{19}F nuclei are shielded in hydrazones **1** and deshielded in azo **2** by electron-withdrawing substituents. Detailed analysis of chemical shifts in both series of compounds demonstrated that they correlate with the substituent Hammett σ_p parameter.¹¹ The correlation is clearly non-linear and can be fitted to a quadratic function. Interestingly, the orientation of the parabolic fitting curve is different for each series reflecting differences in the mechanisms modulating the electron density around the monitored nuclei: in the hydrazones **1** the sp^2 -hybridized carbon atom is part of the conjugated array of atoms to which the fluorine atoms are hyper-conjugated, while in the azo tautomers **2** the π conjugation stops at the nitrogen atom (Fig. 7).

Quantitative analysis of the results in Table 1 demonstrates that the log of experimental K_{exp} values correlate well with substituent parameters σ_p (Fig. 8). Two datapoints, for H (**d**) and Me (**c**), appear to fit poorly the correlation, although they follow the trend in the series. When they are excluded, the remaining datapoints are well fitted into a linear function with a high correlation factor r^2 . Similar analysis of the DFT-calculated equilibrium constant values K_{theor} also demonstrates a linear correlation with σ_p values. For the best linear fit, two theoretical datapoints were excluded from the correlation. Interestingly, datapoints poorly fitting the theoretical correlation are π donors, MeO (**b**) and F (**e**), while in fitting the experimental data two sigma donors, Me (**c**) and H (**d**) are outside the correlation. A comparison of the two fitting lines in Fig. 8 shows that DFT calculations excessively favor the hydrazono tautomer by a factor of about 50 ($\Delta\log \approx 1.7$) relative to the experimental results.

The observed trends and correlations are consistent with resonance forms and charge delocalization shown for both tautomers in Fig. 7: the electron-withdrawing substituents X are good acceptors of the lone pair of the hydrazono group in **1**, while the azo group in **2** is a good acceptor of electron density from the electron donating

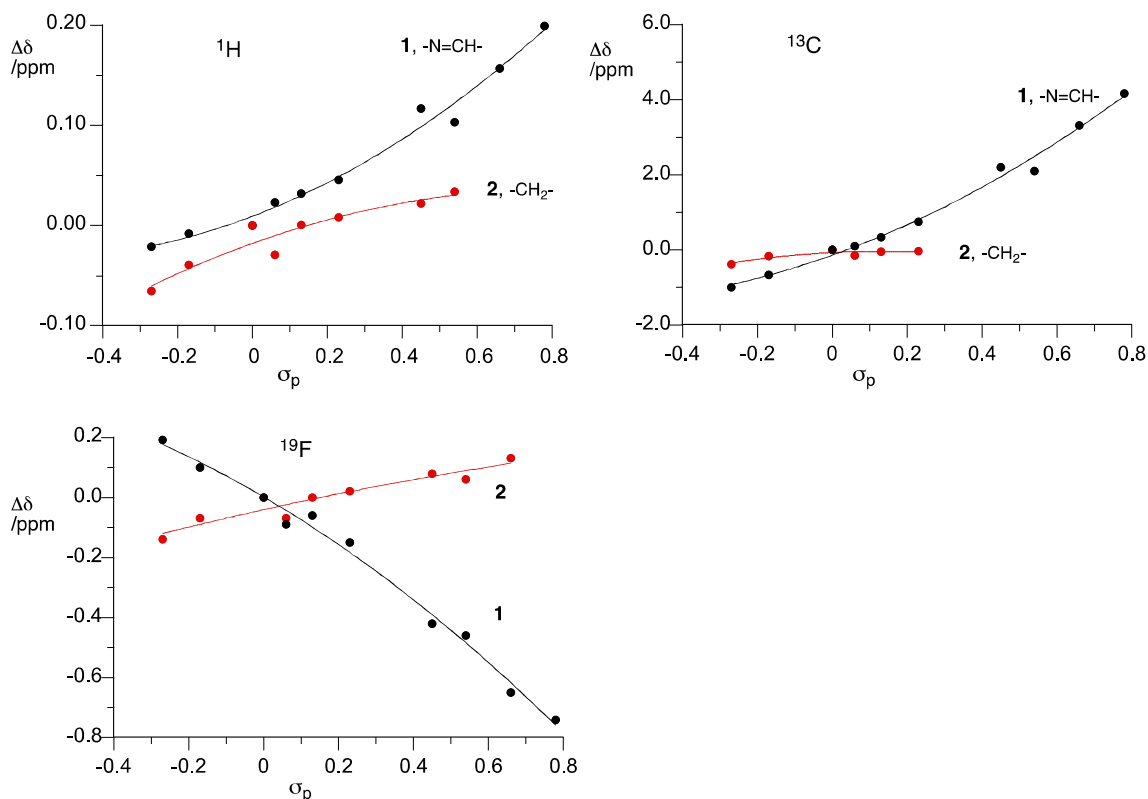


Fig. 6. Correlation of the difference in ^1H , ^{13}C , and ^{19}F chemical shifts ($\Delta\delta = \delta_x - \delta_H$) for series of hydrazones **1** (black) and azo derivatives **2** (red).

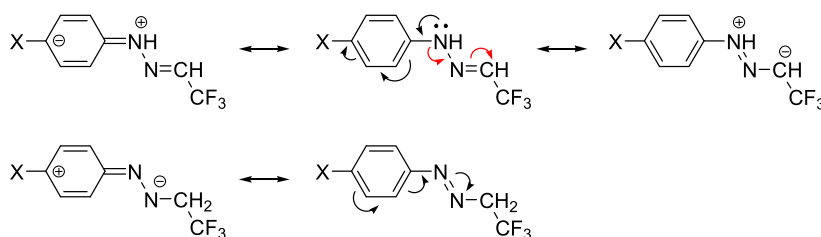


Fig. 7. Selected resonance structures for **1** and **2**.

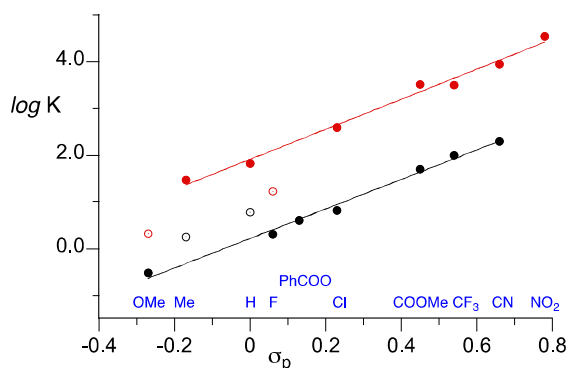


Fig. 8. A plot of experimental (black) and calculated (red) equilibrium constants K for **1**–**2** against substituent parameter σ_p . Best fitting lines without the open-circle datapoints: $\log K_{\text{exp}} = 3.15 \times \sigma_p + 0.22$, $r^2 = 0.99$; $\log K_{\text{theor}} = 3.21 \times \sigma_p + 1.91$, $r^2 = 0.99$.

groups X. As evident from the DFT optimized geometry of **1d** and **2d**, the azo and hydrazo groups are co-planar with the benzene ring allowing for full conjugation (Fig. 9).

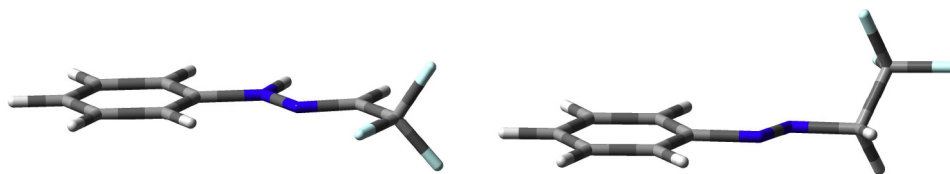


Fig. 9. Molecular geometry for **1d** (left) and **2d** (right) obtained at the M062X/6-31G(2d,p) level of theory.

The position of the tautomeric equilibrium for trifluoroacetaldehyde *p*-tolylhydrazone (**1c**) was investigated in several solvents at ambient temperature by ^1H NMR spectroscopy and chemical shifts are listed in Table 2. The equilibrium **1c**–**2c** was reached within 8–10 h in CDCl_3 and CD_2Cl_2 solvents, 1 day for CD_3CN , and the slowest appearance of the azo tautomer was observed for benzene (4 days) and DMSO-d_6 solutions (1 week). In another experiment, a ~2:1 mixture of tautomers **1c**–**2c** (obtained after evaporation of the solvent from equilibrated mixture in CDCl_3 solution) was kept in DMSO-d_6 to give almost pure hydrazone tautomer after 6 days.

Table 2
Chemical shifts δ (ppm) in ^1H NMR spectra of **1c** and **2c** in different solvents

Tautomeric	Solvent	Chemical shifts δ (ppm)						$J_{\text{H-F}}$ (Hz)
		1-H	N-H	2'-H	3'-H	CH_3		
1c	CDCl_3	6.92	7.89	7.10	6.98	2.30	4.1	
	CD_2Cl_2	6.97	8.03	7.12	6.98	2.29	4.2	
	C_6D_6	5.81	6.55	6.92	6.80	2.09	4.2	
	CD_3CN	7.12	9.15	7.11	6.96	2.26	4.4	
	DMSO-d_6	7.26	10.97	7.08	6.94	2.22	4.5	
2c	CDCl_3	4.46	—	7.66	7.28	2.42	9.7	
	CD_2Cl_2	4.48	—	7.66	7.31	2.42	9.8	
	C_6D_6	3.99	—	7.69	6.88	1.97	9.8	
	CD_3CN	4.57	—	7.64	7.35	2.41	10.1	
	DMSO-d_6	4.81	—	7.63	7.38	2.39	10.5	

The observed behavior of **1c** in various solvents is consistent with acid-catalyzed tautomerization. Thus, in commercial chlorinated solvents, the tautomeric interconversion is accelerated by the residual acid (DCI). As expected, exposure of freshly prepared solutions of **1c** to HCl vapors resulted in reaching the equilibrium points within a few minutes and the resulting equilibrium constants K are listed in Table 3.

Table 3
Experimental and calculated equilibrium constant K for **1c**–**2c** in selected solvents at room temperature

Solvent	K_{exp}	K_{theor}	ϵ	$E_{\text{T}(30)}$
CDCl_3	1.8	29.2	4.7	39.1
CD_2Cl_2	3.3	50.9	8.9	40.7
CD_3CN	32.3	89.0	35.7	45.6
DMSO	49.0	93.5	46.8	45.1
C_6D_6	4.9	11.3	2.3	34.3

Results shown in Table 3 demonstrate that, with the exception of benzene, increasing dielectric strength of the solvent increasingly favors the hydrazone tautomer **1c** over the azo **2c**. Quantitative analysis shows that the four experimental values K_{exp} and six calculated equilibrium constants K_{theor} correlate well with the solvent parameter $E_{\text{T}(30)}$ (Fig. 10).² One possible reason for the experimental datapoint for benzene solution being significantly off the correlation, is related to specific solvation and π – π interactions of the solvent with one of the tautomers. The observed distribution of tautomers in equilibrium is due to higher dielectric dipole mo-

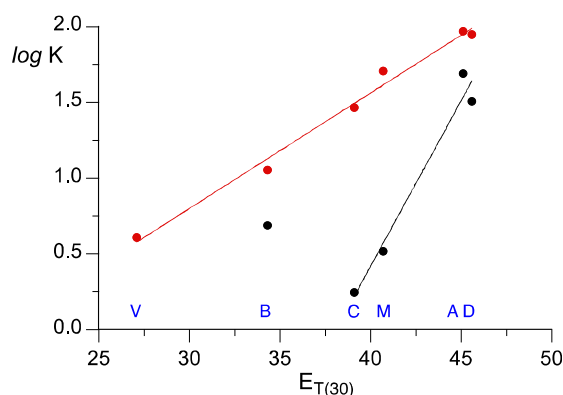
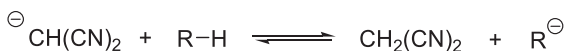


Fig. 10. A plot of experimental (black) and theoretical data (red) for $\log(K)$ of **1c**–**2c** versus solvent parameter $E_{\text{T}(30)}$: V—vacuum, B—benzene, C—chloroform, M—methylene chloride, A—acetonitrile, D—dimethyl sulfoxide. Best fit line: experimental without B, $\log K_{\text{exp}} = 0.218 \times E_{\text{T}(30)} - 8.32$, $r^2 = 0.97$; theoretical $\log K_{\text{theor}} = 0.076 \times E_{\text{T}(30)} - 1.49$, $r^2 = 0.988$.

ment of the hydrazone form **1c** (3.52 D calculated in vacuum) than the azo tautomer **2c** (2.87 D in vacuum) and its greater stabilization in polar solvents.

Although the tautomerization of **1** to **2** is an acid-catalyzed process, interestingly, hydrazone **1d** does not tautomerize to **2d** under the reaction conditions used by Rueping^{7h} for construction of the pyridazine ring. Thus, ^1H NMR analysis of a mixture of **1d**, AcOH (0.4 equiv), and proline (0.2 equiv) in CD_2Cl_2 at ambient temperature revealed no traces of **2d** even after 24 h. This indicates that the acetic acid is too weak to effect tautomerization and that the nucleophilicity of the hydrazone **1d** is solely due to the resonance form shown in Fig. 2, rather than deprotonation of the azo form.

To assess the acidity of the azo tautomer **1d**, acid–base equilibrium reactions for malononitrile ($\text{p}K_{\text{a}} = 11.0$)¹² with **1d** and several other known C–H acids were investigated with the DFT methods in DMSO dielectric medium, as shown in Scheme 2. A comparison of computational and experimental¹² results for four



Scheme 2. Acid–base equilibrium for malononitrile and C–H acids.

model compounds (Table 4) demonstrates that the calculated pK_a values are generally higher by a couple of pK_a units, but otherwise in fairly good agreement with the experimental data, considering that some conformational and tautomeric effects are not fully implemented in the modeling. Similar analysis for azo compound **2d** shows the calculated pK_a value of 16.3, which is lower than that calculated for diethyl malonate (17.7). Interestingly, substitution of the COOEt for CF_3 in **2d** has a marked effect on acidity and ethyl phenylazoacetate has a pK_a value similar to that of malononitrile (Table 4). Thus, the acidity of the azo tautomer **2d** is similar to that of a malonate ester and suggests that the anion could be generated under mild conditions offering a new synthetically useful intermediate.

Table 4
Calculated and experimental pK_a values in DMSO for selected compounds

acid	pK_a	
	Calcd ^a	Exp ^b
$\text{CH}_2(\text{COOEt})_2$	17.7	16.4
$\text{PhCH}_2\text{COOEt}$	24.9	22.6
$\text{PhCH}=\text{NNHPh}$	22.7	21.1
$\text{PhCH}=\text{NCH}_2\text{COOEt}$	19.5	19.5
$\text{PhN}=\text{NCH}_2\text{COOEt}$	11.3	—
$\text{PhN}=\text{NCH}_2\text{CF}_3$	16.3	—

^a $pK_a(\text{R-H}) = \Delta G_{298}/RT + 11.0$. ΔG_{298} for the equilibrium reaction in Scheme 2 was calculated with M06-2x/6-31+G(2d,p)//M06-2x/6-31G(2d,p) level of theory with the PCM solvation model (DMSO).

^b From Ref. 12.

3. Conclusions

Results demonstrate that the CF_3 group provides an appropriate balance of the electronic structure, such that both tautomeric forms, hydrazono and azo, are observed at equilibrium. The equilibration of the tautomers is an acid-catalyzed process, which occurs slowly with natural concentration of acid in chlorinated solvents, and much more rapidly upon exposure to HCl vapors. Weaker acids, such as AcOH are ineffective for the tautomerization process. Chemical shifts of diagnostic nuclei and position of the equilibrium are conveniently investigated by correlation analysis with substituent parameters and well modeled by DFT methods. Results of correlation analysis of the NMR data are consistent with different mechanisms of modulation of electron density around the nuclei in the hydrazono and azo series. The position of the hydrazono-azo equilibrium depends on the solvent polarity, presumably due to the difference in the molecular dipole moments of the two forms.

Acid-catalyzed tautomerization of easily available hydrazones **1** provides convenient access to azo tautomers **2** that might be important building blocks for construction of the pyridazine skeleton via the hetero-Diels–Alder process. The azo tautomers are also predicted to be relatively acidic, which suggests their possible synthetic applications in the carbanion chemistry.

4. Computational details

Quantum-mechanical calculations were carried out using the Gaussian 09 suite of programs.¹³ Geometry optimizations for unconstrained tautomers were undertaken at the M062X/6-31G(2d,p) level of theory¹⁴ using tight convergence limits. Only *trans*-azo derivatives **2** were considered in accordance to experimental observations, and all compounds were subjected to limited conformational search for the global minima. Zero point energies were

scaled by 0.9806.¹⁵ Calculations in solvent dielectric media were performed at the M062X/6-31+G(2d,p)//M062X/6-31G(2d,p) level of theory using the PCM model¹⁶ requested with the SCRF(Solvent=name) keyword.

5. Experimental part

5.1. General

Solvents and reagents were purchased and used as received without further purification. Products were purified by flash chromatography on silica gel (230–400 mesh, Merck or Fluka). Unless stated otherwise, yields refer to analytically pure samples. NMR spectra were recorded on a Bruker AVIII 600 instrument. Chemical shifts are reported relative to solvent residual peaks (¹H NMR: $\delta=1.94$ ppm [CD_3CN], $\delta=2.50$ ppm [DMSO-*d*₆], $\delta=5.32$ ppm [CD_2Cl_2], $\delta=7.16$ ppm [C_6D_6], $\delta=7.26$ ppm [CDCl_3]; ¹³C NMR: $\delta=77.0$ ppm [CDCl_3]).¹⁷ For detailed peak assignments 2D spectra were measured (COSY, HMQC, HMBC). IR spectra were measured with an FTIR NEXUS spectrometer (as KBr pellets or thin films). MS were performed with a Finnigan MAT-95 or a Varian 500-MS LC Ion Trap instrument. UV–vis were measured on Perkin Elmer Lambda 45 spectrometer. Elemental analyses were obtained with a Vario EL III (Elementar Analysensysteme GmbH) instrument. Melting points were determined in capillaries with a SMP30 apparatus (Stuart) or with a MEL-TEMP II apparatus (Aldrich) and are uncorrected.

5.2. Starting materials

Hydrazines **3b–e,g,i–k** are commercially available (TCI, Aldrich) as hydrochloride salts or as a free base (**3i**). Methyl 4-hydrazinobenzoate (**3h**) was prepared according to a literature protocol.¹⁸ The syntheses of phenylhydrazine derivatives **3a** and **3f** were described elsewhere.¹⁹ Trifluoroacetaldehyde hydrate (**4**, 72% aq) was purchased from Fluorochem, and used as received.

5.3. UV–vis measurement

Electronic absorption spectra of **1a** and **2a** were obtained for three concentrations in a range of $1.8\text{--}7.5 \times 10^{-5}$ mol/L in acetonitrile, and maximum absorption at about 290 nm was fitted to Beer's law.

5.4. Quantification in NMR experiments

The relative concentration of tautomers was established by integrations of signals attributed to azomethine proton ($\text{N}=\text{CHCF}_3$) and methylene protons (CH_2CF_3) for all tautomeric pairs with the exception of **1a/2a** and **1h/2h** pairs: in the former benzylic and in the latter methoxy protons were used for establishing the tautomeric ratio.

5.5. Sample preparation for HCl-induced equilibration of tautomers

NMR tubes containing solutions of ca. 3 mg of **1c** in 0.6 mL of appropriate solvent were exposed to HCl vapors in a closed Erlenmeyer flask (filled with a thin layer of concd HCl at the bottom) for 15 min, and the ¹H NMR spectra were taken immediately.

5.6. General procedure for the synthesis of tri-fluoroacetaldehyde hydrazones **1a–1k**

A mixture of the appropriate hydrazine hydrochloride **3** (1.0 mmol), fluoral hydrate (ca. 3.0 mmol), freshly dried and crushed molecular sieves 4 Å (**4**, 0.42 g) in MeOH (3.5 mL) was

heated overnight at 75 °C in a closed ampoule. The resulting mixture was cooled to room temp, diluted with DCM (15 mL), and filtered through Celite. The filtrate was extracted with H₂O, the organic layer was washed with 5% aq NaHCO₃, and water (2×25 mL). The organic layer was dried (Na₂SO₄), filtered, and solvents were removed under reduced pressure (cold bath) to afford spectroscopically pure products **1**. Analytically pure samples were obtained either by flash chromatography or by recrystallization.

5.6.1. Trifluoroacetaldehyde 4-benzyloxyphenylhydrazone (1a).⁹ Crude product was recrystallized from pentane/methanol (dry ice temperature) to give **1a** (238 mg, 81% yield) as a pale yellow solid; mp 116–118 °C; ¹H NMR (CDCl₃, 600 MHz): δ 5.04 (s, 2H, Bn), 6.91 (qd, J_{H-H}=1.4 Hz, J_{H-F}=4.1 Hz, 1H, =CHCF₃), 6.94, 7.02 (2 d, J=9.0 Hz each, 2H each), 7.31–7.44 (m, 5H), 7.83 (br s, 1H, NH) ppm; UV (MeCN), λ_{max} (log ε) 290 (4.26), 319sh (4.00), 500 (1.80). ¹³C, ¹⁹F NMR, IR, and MS of **1a** are consistent with those reported.⁹ Filtration of **1a** through a short silica gel pad (DCM) gave a small sample of pure **2a** in ca. 30% yield: mp 63–65 °C; ¹H NMR (CDCl₃, 600 MHz): δ 4.43 (q, J_{H-F}=9.7 Hz, 2H, CH₂CF₃), 5.14 (s, 2H, Bn), 7.05 (d, J=9.0 Hz, 2H), 7.33–7.45 (m, 5H), 7.76 (d, J=9.0 Hz, 2H) ppm; ¹³C NMR (CDCl₃, 150 MHz): δ 68.5 (q, ²J_{C-F}=28.4 Hz, CH₂CF₃), 70.3 (t, Bn), 124.3 (q, ¹J_{C-F}=277.4 Hz, CF₃), 115.1, 124.7, 127.4, 128.2, 128.7 (5d, 9 arom. CH), 136.3, 146.2, 161.8 (3s, 3i-C) ppm; ¹⁹F NMR (CDCl₃, 565 MHz): δ -68.2 (t, J_{H-F}=9.7 Hz, CF₃) ppm; UV (MeCN), λ_{max} (log ε) 290 (4.29), 318sh (4.13), 390sh (2.56), 500 (2.12). IR (KBr): ν 1380 (N=N), 1255, 1160 (C=O), 1160–1110 (CF₃) cm⁻¹; EIMS (m/z): 294 (32, [M]⁺), 203 (57, [M-Bn]⁺), 91 (100, [Bn]⁺). Anal. Calcd for C₁₅H₁₃F₃N₂O (294.1): C 61.22, H 4.45. Found: C 61.24, H 4.73.

5.6.2. Trifluoroacetaldehyde 4-methoxyphenylhydrazone (1b). Crude product was recrystallized from petroleum ether (dry ice temperature) to give **1b** (241 mg, 55% yield) as a light orange solid; mp 74–76 °C; ¹H NMR (CDCl₃, 600 MHz): δ 3.79 (s, 3H, OMe), 6.86 (d, J=9.0 Hz, 2 arom. CH), 6.90 (q_{br}, J_{H-F}=4.1 Hz, 1H, =CHCF₃), 7.02 (d, J=9.0 Hz, 2 arom. CH), 7.86 (br s, 1H, NH) ppm; ¹³C NMR (CDCl₃, 150 MHz): δ 55.6 (q, OMe), 114.8, 115.3 (2d, 4 arom. CH), 121.2 (q, ¹J_{C-F}=268.8 Hz, CF₃), 121.3 (q, ²J_{C-F}=39.0 Hz, =CHCF₃), 136.3, 155.4 (2s, 2i-C) ppm; ¹⁹F NMR (CDCl₃, 565 MHz): δ -65.2 (d, J_{H-F}=4.1 Hz, CF₃) ppm; IR (KBr): ν 3310 (N-H), 1610 (C=N), 1295, 1245 (C=O), 1245–1105 (CF₃) cm⁻¹; EIMS (m/z): 218 (54, M⁺), 122 (100, [M-NCHCF₃]⁺). Anal. Calcd for C₉H₉F₃N₂O (218.1): C 49.55, H 4.16. Found: C 49.74, H 4.20.

Data for azo tautomer 2b (in a mixture with 1b): ¹H NMR (CDCl₃, 600 MHz): δ 3.88 (s, 3H, OMe), 4.43 (q, J_{H-F}=9.7 Hz, 2H, CH₂CF₃), 6.97, 7.76 (2d, J=9.0 Hz, 2H each) ppm; ¹³C NMR (CDCl₃, 150 MHz): δ 55.6 (q, OMe), 68.5 (q, ²J_{C-F}=28.3 Hz, CH₂CF₃), 114.2 (d, 2 arom. CH), 124.3 (q, ¹J_{C-F}=277.3 Hz, CF₃), 124.7 (d, 2 arom. CH), 146.0, 162.6 (2s, 2i-C) ppm; ¹⁹F NMR (CDCl₃, 565 MHz): δ -68.2 (t, J_{H-F}=9.7 Hz, CF₃) ppm.

5.6.3. Trifluoroacetaldehyde p-tolylhydrazone (1c).²⁰ Crude product was flash chromatographed (SiO₂, petroleum ether/DCM 3:2) to give **1c** (141 mg, 70% yield) as a light orange solid; mp 74–76 °C; ¹H NMR (CDCl₃, 600 MHz): δ 2.30 (s, 3H, Me), 6.92 (qd, J_{H-H}=1.1 Hz, J_{H-F}=4.1 Hz, 1H, =CHCF₃), 6.98, 7.10 (2d, J=8.4 Hz, 2H each), 7.89 (br s, 1H, NH) ppm; ¹³C NMR (CDCl₃, 150 MHz): δ 20.6 (q, Me), 113.6 (d, 2 arom. CH), 121.1 (q, ¹J_{C-F}=268.9 Hz, CF₃), 121.7 (q, ²J_{C-F}=39.0 Hz, =CHCF₃), 129.9 (d, 2 arom. CH), 131.7, 140.3 (2s, 2i-C) ppm; ¹⁹F NMR (CDCl₃, 565 MHz): δ -65.3 (d, J_{H-F}=4.1 Hz, CF₃) ppm; IR (KBr): ν 3310 (N-H), 1620 (C=N), 1135–1110 (CF₃) cm⁻¹; (-)ESI-MS (m/z): 201 (100, [M-H]⁻). Anal. Calcd for C₉H₉F₃N₂ (202.1): C 53.47, H 4.49, N 13.86. Found: C 53.22, H 4.51, N 13.72.

Data for azo tautomer 2c (in a mixture with 1c): ¹H NMR (CDCl₃, 600 MHz): δ 2.42 (s, 3H, Me), 4.46 (q, J_{H-F}=9.7 Hz, 2H, CH₂CF₃), 7.28, 7.66 (2d, J=8.2 Hz, 2H each) ppm; ¹³C NMR (CDCl₃, 150 MHz): δ 21.4

(q, Me), 68.7 (q, ²J_{C-F}=28.5 Hz, CH₂CF₃), 122.7 (d, 2 arom. CH), 124.2 (q, ¹J_{C-F}=277.5 Hz, CF₃), 129.7 (d, 2 arom. CH), 142.5, 149.8 (2s, 2i-C) ppm; ¹⁹F NMR (CDCl₃, 565 MHz): δ -68.1 (t, J_{H-F}=9.7 Hz, CF₃) ppm.

5.6.4. Trifluoroacetaldehyde phenylhydrazone (1d).²¹ Crude product was flash chromatographed (SiO₂, petroleum ether/DCM 3:2) to give **1d** (177 mg, 94% yield) as an orange solid; mp 48–50 °C; ¹H NMR (CDCl₃, 600 MHz): δ 6.93 (br q, J_{H-F}=4.0 Hz, 1H, =CHCF₃), 6.98–7.02, 7.07–7.10, 7.29–7.33 (3 m, 1H, 2H, 2H), 7.92 (br s, 1H, NH) ppm; ¹³C NMR (CDCl₃, 150 MHz): δ 113.5 (d, 2 arom. CH), 121.0 (q, ¹J_{C-F}=269.1 Hz, CF₃), 122.2 (d, arom. CH), 122.3 (q, ²J_{C-F}=39.0 Hz, =CHCF₃), 129.4 (d, 2 arom. CH), 142.6 (s, i-C) ppm; ¹⁹F NMR (CDCl₃, 565 MHz): δ -65.4 (d, J_{H-F}=4.0 Hz, CF₃) ppm; IR (KBr): ν 3320 (N-H), 1620 (C=N), 1605 (C=C), 1160–1070 (CF₃) cm⁻¹; EIMS (m/z): 188 (100, M⁺), 119 (28, [M-CF₃]⁺). Anal. Calcd for C₈H₇F₃N₂ (188.1): C 51.07, H 3.75. Found: C 51.04, H 3.74.

Data for azo tautomer 2d (in a mixture with 1d): ¹H NMR (CDCl₃, 600 MHz): δ 4.50 (q, J_{H-F}=9.8 Hz, 2H, CH₂CF₃), 7.48–7.52, 7.76–7.79 (2m, 3H, 2H) ppm; ¹³C NMR (CDCl₃, 150 MHz): δ 68.8 (q, ²J_{C-F}=28.6 Hz, CH₂CF₃), 122.7 (d, 2 arom. CH), 124.2 (q, ¹J_{C-F}=277.4 Hz, CF₃), 129.1, 131.8 (2d, 3 arom. CH), 151.7 (s, i-C) ppm; ¹⁹F NMR (CDCl₃, 565 MHz): δ -68.0 (t, J_{H-F}=9.8 Hz, CF₃) ppm.

5.6.5. Trifluoroacetaldehyde 4-fluorophenylhydrazone (1e). Crude product was flash chromatographed (SiO₂, petroleum ether/DCM 1:2) to give **1e** (169 mg, 82% yield) as an orange solid; mp 34–35 °C; ¹H NMR (CDCl₃, 600 MHz): δ 6.96 (qd, J_{H-H}=1.3 Hz, J_{H-F}=4.0 Hz, 1H, =CHCF₃), 6.98–7.05 (m, 4H), 7.91 (br s, 1H, NH) ppm; ¹³C NMR (CDCl₃, 150 MHz): δ 114.8 (d, ²J_{C-F}=7.8 Hz, 2 arom. CH), 116.0 (d, ²J_{C-F}=22.9 Hz, 2 arom. CH), 121.0 (q, ¹J_{C-F}=269.1 Hz, CF₃), 122.4 (q, ²J_{C-F}=39.2 Hz, =CHCF₃), 138.9 (d, ⁴J_{C-F}=2.2 Hz, i-C-N), 158.5 (d, ¹J_{C-F}=240.4 Hz, i-C-F) ppm; ¹⁹F NMR (CDCl₃, 565 MHz): δ -121.9 (m, Ar-F), -65.5 (d, J_{H-F}=4.0 Hz, CF₃) ppm; IR (KBr): ν=3360 (N-H), 1600 (C=N, C=C), 1505, 1140–1095 (CF₃) cm⁻¹; CIMS (m/z): 206 (100, M⁺), 110 (67, [M-NCHCF₃]⁺). Anal. Calcd for (%) for C₈H₆F₄N₂ (206.0): C 46.61, H 2.93. Found: C 46.68, H 2.87.

Data for azo tautomer 2e (in a mixture with 1e): ¹H NMR (CDCl₃, 600 MHz): δ 4.47 (q, J_{H-F}=9.6 Hz, 2H, CH₂CF₃), 7.14–7.18, 7.77–7.81 (2 m, 2H each) ppm; ¹³C NMR (CDCl₃, 150 MHz): δ 68.7 (q, ²J_{C-F}=28.7 Hz, CH₂CF₃), 116.1 (d, ²J_{C-F}=23.0 Hz, 2 arom. CH), 124.1 (q, ¹J_{C-F}=277.4 Hz, CF₃), 124.9 (d, ³J_{C-F}=9.2 Hz, 2 arom. CH), 148.2 (d, ⁴J_{C-F}=2.9 Hz, i-C-N), 164.9 (d, ¹J_{C-F}=253.1 Hz, i-C-F) ppm; ¹⁹F NMR (CDCl₃, 565 MHz): δ -107.9 (m, Ar-F), -68.1 (t, J_{H-F}=9.6 Hz, CF₃) ppm.

5.6.6. Trifluoroacetaldehyde 4-benzyloxyphenylhydrazone (1f).⁹ Crude product was flash chromatographed (SiO₂, DCM) to give **1f** (262 mg, 85% yield) as a yellow solid; mp 165–167 °C (hexanes/CHCl₃); ¹H NMR (CDCl₃, 600 MHz): δ 6.96 (qd, J_{H-H}=1.0 Hz, J_{H-F}=4.1 Hz, 1H, =CHCF₃), 7.04–7.08, 7.10–7.13, 7.51–7.54 (3m, 2H each), 7.63–7.67 (m, 1H), 8.18 (br s, 1H, NH), 8.20–8.22 (m, 2H) ppm; ¹³C, ¹⁹F NMR, IR, and MS of **1f** are consistent with those reported.⁹

Data for azo tautomer 2f (in a mixture with 1f): ¹H NMR (CDCl₃, 600 MHz): δ 4.50 (q, J_{H-F}=9.6 Hz, 2H, CH₂CF₃), 7.36 (d, J=8.8 Hz, 2H), 7.52–7.56, 7.65–7.68 (2m, 2H, 1H), 7.86 (d, J=8.8 Hz, 2H), 8.20–8.23 (m, 2H) ppm; ¹³C NMR (CDCl₃, 150 MHz): δ 68.8 (q, ²J_{C-F}=28.7 Hz, CH₂CF₃), 122.6 (d, 2 arom. CH), 124.1 (q, ¹J_{C-F}=277.4 Hz, CF₃), 124.2, 128.7, 129.1, 130.3, 133.9, 149.3, 153.7 (2d, s, 2d, 2s), 164.8 (s, C=O) ppm; ¹⁹F NMR (CDCl₃, 565 MHz): δ -68.0 (t, J_{H-F}=9.6 Hz, CF₃) ppm.

5.6.7. Trifluoroacetaldehyde 4-chlorophenylhydrazone (1g). Crude product was flash chromatographed (SiO₂, petroleum ether/DCM 1:1) to give **1g** (151 mg, 68% yield) as an orange crystals; mp 40–42 °C; ¹H NMR (CDCl₃, 600 MHz): δ 6.98 (qd, J_{H-H}=1.3 Hz, J_{H-F}=4.0 Hz, 1H, =CHCF₃), 7.04, 7.28 (2d, J=8.8 Hz, 2H each), 7.94 (br s, 1H, NH) ppm; ¹³C NMR (CDCl₃, 150 MHz): δ 114.7 (d, 2 arom. CH), 120.9 (q, ¹J_{C-F}=269.3 Hz, CF₃), 123.1 (q, ²J_{C-F}=39.2 Hz, =CHCF₃),

129.4 (d, 2 arom. CH), 129.4, 141.4 (2s, 2i-C) ppm; ^{19}F NMR (CDCl_3 , 565 MHz): δ -65.6 (d, $J_{\text{H-F}}=4.0$ Hz, CF_3) ppm; IR (KBr): ν 3325 (N–H), 1620, 1595 (C=N, C=C), 1490, 1290, 1245, 1140–1090 (CF_3) cm^{-1} ; EIMS (m/z): 222 (100, M^+), 126 (49, $[\text{M}-\text{NCHCF}_3]^+$), 99 (23). Anal. Calcd for $\text{C}_8\text{H}_6\text{ClF}_3\text{N}_2$ (222.0): C 43.17, H 2.72. Found: C 43.42, 2.57.

Data for azo tautomer **2g** (in a mixture with **1g**): ^1H NMR (CDCl_3 , 600 MHz): δ 4.51 (q, $J_{\text{H-F}}=9.6$ Hz, 2H, CH_2CF_3), 7.49, 7.74 (2d, $J=8.7$ Hz, 2H each) ppm; ^{13}C NMR (CDCl_3 , 150 MHz): δ 68.8 (q, $J_{\text{C-F}}=28.9$ Hz, CH_2CF_3), 124.1 (q, $J_{\text{C-F}}=277.4$ Hz, CF_3), 124.0, 127.0 (2d, 4 arom. CH), 138.0, 150.0 (2s, 2i-C) ppm; ^{19}F NMR (CDCl_3 , 565 MHz): δ -68.0 (t, $J_{\text{H-F}}=9.6$ Hz, CF_3) ppm.

5.6.8. Trifluoroacetaldehyde 4-methoxycarbonylphenylhydrazone (**1h**). Crude product was flash chromatographed (SiO_2 , DCM) to give **1h** (89 mg, 38% yield) as a light orange solid; mp 176–178 °C; ^1H NMR (CDCl_3 , 600 MHz): δ 3.89 (s, 3H, OMe), 7.04 (qd, $J_{\text{H-H}}=1.4$ Hz, $J_{\text{H-F}}=3.9$ Hz, 1H, $=\text{CHCF}_3$), 7.11, 7.99 (2d, $J=8.8$ Hz, 2H each), 8.19 (br s, 1H, H, NH) ppm; ^{13}C NMR (CDCl_3 , 150 MHz): δ 51.9 (q, OMe), 112.8 (d, 2 arom. CH), 120.7 (q, $J_{\text{C-F}}=269.7$ Hz, CF_3), 123.8 (s, i-C), 124.5 (q, $J_{\text{C-F}}=39.4$ Hz, $=\text{CHCF}_3$), 131.5 (d, 2 arom. CH), 146.3 (s, i-C), 166.8 (s, C=O) ppm; ^{19}F NMR (CDCl_3 , 565 MHz): δ -65.8 (d, $J_{\text{H-F}}=3.9$ Hz, CF_3) ppm; IR (KBr): ν 3280 (N–H), 1690 (C=O), 1595 (C=N), 1250, 1170 (C–O), 1125–1095 (CF_3) cm^{-1} ; EI-HRMS: calcd for $\text{C}_{10}\text{H}_9\text{F}_3\text{N}_2\text{O}_2$ [M^+] 246.0616; found 246.0623. Diagnostics signal for azo tautomer **2h** (in a mixture with **1h**): ^1H NMR (CDCl_3 , 600 MHz): δ 4.52 (q, $J_{\text{H-F}}=9.6$ Hz, 2H, CH_2CF_3).

5.6.9. Trifluoroacetaldehyde 4-trifluoromethylphenylhydrazone (**1i**). Crude product was flash chromatographed (SiO_2 , petroleum ether/DCM 1:1) to give **1i** (169 mg, 66% yield) as a yellow oil; ^1H NMR (CDCl_3 , 600 MHz): δ 7.03 (qd, $J_{\text{H-H}}=1.3$ Hz, $J_{\text{H-F}}=4.0$ Hz, 1H, $=\text{CHCF}_3$), 7.15, 7.55 (2d, $J=8.6$ Hz, 2H each), 8.08 (br s, 1H, NH) ppm; ^{13}C NMR (CDCl_3 , 150 MHz): δ 113.1 (d, 2 arom. CH), 120.7 (q, $J_{\text{C-F}}=269.6$ Hz, CF_3), 124.1 (q, $J_{\text{C-F}}=32.7$ Hz, i-C), 124.3 (q, $J_{\text{C-F}}=271.1$ Hz, CF_3), 124.4 (q, $J_{\text{C-F}}=39.5$ Hz, N= CHCF_3), 126.8 (q, $J_{\text{C-F}}=3.8$ Hz, 2 arom. CH), 145.3 (s, i-C) ppm; ^{19}F NMR (CDCl_3 , 565 MHz): δ -65.9 (d, $J_{\text{H-F}}=4.0$, CF_3), -61.8 (s, Ar- CF_3) ppm; IR (KBr): ν 3360 (N–H), 1615 (C=N), 1180–1065 (CF_3) cm^{-1} ; CIMS (m/z): 257 (100, $[\text{M}+\text{H}]^+$), 256 (83, M^+), 237 (22, $[\text{M}-\text{F}]^+$), 201 (17). Anal. Calcd for $\text{C}_9\text{H}_6\text{F}_6\text{N}_2$ (256.0): C 42.20, H 2.36. Found: C 42.15, H 2.19. Diagnostics signal for azo tautomer **2i** (in a mixture with **1i**): ^1H NMR (CDCl_3 , 600 MHz): δ 4.53 (q, $J_{\text{H-F}}=9.6$ Hz, 2H, CH_2CF_3).

5.6.10. Trifluoroacetaldehyde 4-cyanophenylhydrazone (**1j**). Crude product was flash chromatographed (SiO_2 , DCM) to give **1j** (179 mg, 84% yield) as a colorless solid; mp 146–148 °C; ^1H NMR (CDCl_3 , 600 MHz): δ 7.09 (qd, $J_{\text{H-H}}=1.4$ Hz, $J_{\text{H-F}}=4.0$ Hz, 1H, $=\text{CHCF}_3$), 7.15, 7.58 (2d, $J=8.8$ Hz, 2H each), 8.29 (br s, 1H, NH) ppm; ^{13}C NMR (CDCl_3 , 150 MHz): δ 104.7 (s, CN), 113.6 (d, 2 arom. CH), 119.2 (s, i-C), 120.5 (q, $J_{\text{C-F}}=269.9$ Hz, CF_3), 125.6 (q, $J_{\text{C-F}}=39.5$ Hz, $=\text{CHCF}_3$), 133.8 (d, 2 arom. CH), 146.2 (s, i-C) ppm; ^{19}F NMR (CDCl_3 , 565 MHz): δ -66.1 (d, $J_{\text{H-F}}=4.0$, CF_3) ppm; IR (KBr): ν 3255 (N–H), 2230 (C≡N), 1600 (C=N), 1140–1100 (CF_3) cm^{-1} ; CIMS (m/z): 214 (100, $[\text{M}+\text{H}]^+$). Anal. Calcd for $\text{C}_9\text{H}_6\text{F}_3\text{N}_3$ (213.0): C 50.71, H 2.84. Found: C 50.83, H 2.72. Diagnostics signal for azo tautomer **2j** (in a mixture with **1j**): ^1H NMR (CDCl_3 , 600 MHz): δ 4.54 (q, $J_{\text{H-F}}=9.6$ Hz, 2H, CH_2CF_3).

5.6.11. Trifluoroacetaldehyde 4-nitrophenylhydrazone (**1k**).²¹ Crude product was flash chromatographed (SiO_2 , DCM) to give **1k** (193 mg, 83% yield) as a pale yellow solid; mp 190–192 °C; ^1H NMR (CDCl_3 , 600 MHz): δ 7.13 (qd, $J_{\text{H-H}}=1.1$ Hz, $J_{\text{H-F}}=3.7$ Hz, 1H, $=\text{CHCF}_3$), 7.17, 8.21 (2d, $J=9.1$ Hz, 2H each), 8.36 (br s, 1H, NH) ppm; ^{13}C NMR (CDCl_3 , 150 MHz): δ 112.9 (d, 2 arom. CH), 120.4 (q,

$J_{\text{C-F}}=269.9$ Hz, CF_3), 125.9 (d, 2 arom. CH), 126.5 (q, $J_{\text{C-F}}=39.6$ Hz, $=\text{CHCF}_3$), 142.4, 147.7 (2s, 2i-C) ppm; ^{19}F NMR (CDCl_3 , 565 MHz): δ -66.2 (d, $J_{\text{H-F}}=3.7$ Hz, CF_3) ppm; IR (KBr): ν 3256 (N–H), 1590 (C=N), 1500, 1335 (N–O), 1125–1090 (CF_3) cm^{-1} ; ESI-MS (m/z): 256 (100, $[\text{M}+\text{Na}]^+$), 234 (44, $[\text{M}+\text{H}]^+$). Diagnostics signal for azo tautomer **2k** (in a mixture with **1k**): ^1H NMR (CDCl_3 , 600 MHz): δ 4.56 (q, $J_{\text{H-F}}=9.5$ Hz, 2H, CH_2CF_3).

Acknowledgements

Support of this work by the National Science Center (NCN 2011/01/BST5/06582 and 2013/09/B/ST5/01230) and the National Science Foundation (NSF CHE-1214104).

References and notes

1. *Tautomerism: Methods and Theories*; Antonov, L., Ed.; Wiley-VCH: Weinheim, Germany, 2013; and references therein.
2. Reichardt, C. *Solvents and Solvent Effects in Organic Chemistry*, 3rd ed.; Wiley-VCH: Weinheim, Germany, 2003; pp 93–120.
3. (a) Fischer, E. *Ber. Dtsch. Chem. Ges.* **1896**, 29, 793–797; (b) Fischer, E. *Ber. Dtsch. Chem. Ges.* **1897**, 30, 1240–1243; (c) Bamberger, E.; Pemsel, W. *Ber. Dtsch. Chem. Ges.* **1903**, 36, 57–84; (d) Kuznetsov, M. A.; Suvorov, A. A. *J. Org. Chem. USSR* **1982**, 18, 1684–1691; (e) Mayr, H.; Grimm, K. *J. Org. Chem.* **1992**, 57, 1057–1059; (f) Ros, A.; Diez, E.; Marqués-López, E.; Martín-Zamora, E.; Vázquez, J.; Iglesias-Sigüenza, J.; Pappalardo, R. R.; Álvarez, E.; Lassaletta, J. M.; Fernández, R. *Tetrahedron: Asymmetry* **2008**, 19, 998–1004; (g) Prechter, A.; Heinrich, M. R. *Synthesis* **2011**, 1515–1525.
4. For better known azo-enol/keto-hydrazone systems equilibrating in a 1,5H-shift fashion, see: (a) Zincke, T.; Bindewald, H. *Ber. Dtsch. Chem. Ges.* **1884**, 17, 3026–3033; (b) Lee, H. Y.; Song, X.; Park, H.; Baik, M.-H.; Lee, D. *J. Am. Chem. Soc.* **2010**, 132, 12133–12144; (c) Duarte, L.; Giuliano, B. M.; Reva, I.; Fausto, R. *J. Phys. Chem. A* **2013**, 117, 10671–10680.
5. (a) Isanbor, C.; O'Hagan, D. *J. Fluorine Chem.* **2006**, 127, 303–319; (b) Bégue, J.-P. *Bioorganic and Medicinal Chemistry of Fluorine*; John Wiley & Sons: Hoboken, NJ, 2008; (c) Salwiczek, M.; Nyakatura, E. K.; Gerling, U. I.; Ye, S.; Koksche, B. *Chem. Rev.* **2012**, 41, 2135–2171; (d) Wang, J.; Sánchez-Roselló, M.; Acena, J. L.; del Pozo, C.; Sorochinsky, A. E.; Fustero, S.; Soloshonok, V. A.; Liu, H. *Chem. Rev.* **2014**, 114, 2432–2506.
6. (a) Kirsch, P. *Modern Fluoroorganic Chemistry, Synthesis, Reactivity, Applications*; Wiley-VCH: Weinheim, Germany, 2004; pp 203–277; (b) Hird, M. *Chem. Soc. Rev.* **2007**, 36, 2070–2095; (c) Berger, R.; Resnati, G.; Metrangolo, P.; Weber, E.; Hulliger, J. *Chem. Soc. Rev.* **2011**, 40, 3496–3508.
7. (a) Tanaka, K.; Suzuki, T.; Maeno, S.; Mitsuhashi, K. *J. Heterocycl. Chem.* **1986**, 23, 1535–1538; (b) Iwata, S.; Namekata, J.; Tanaka, K.; Mitsuhashi, K. *J. Heterocycl. Chem.* **1991**, 28, 1971–1976; (c) Liu, X.; Zou, J.; Fan, Y.; Wang, Q. *Synthesis* **1999**, 1313–1318; (d) Djuric, S. W.; BaMaung, N. Y.; Basha, A.; Liu, H.; Luly, J. R.; Madar, D. J.; Sciotti, R. J.; Tu, N. P.; Wagenaar, F. L.; Wiedeman, P. E.; Zhou, X.; Ballaron, S.; Bauch, J.; Chen, Y.-W.; Chiou, X. G.; Fey, T.; Gauvin, D.; Gubbins, E.; Hsieh, G. C.; Marsh, K. C.; Mollison, K. W.; Pong, M.; Shaughnessy, T. K.; Sheets, M. P.; Smith, M.; Trevillyan, J. M.; Warrior, U.; Wegner, C. D.; Carter, G. W. *J. Med. Chem.* **2000**, 43, 2975–2981; (e) Xie, H.; Zhu, J.; Chen, Z.; Li, S.; Wu, Y. *Synlett* **2012**, 935–937; (f) Das, A.; Volla, C. M. R.; Atodiresei, I.; Bettray, W.; Rueping, M. *Angew. Chem.* **2013**, 125, 8166–8169; *Angew. Chem., Int. Ed.* **2013**, 52, 8008–8011; (g) Wen, J.-J.; Tang, H.-T.; Xiong, K.; Ding, Z.-C.; Zhan, Z.-P. *Org. Lett.* **2014**, 16, 5940–5943; (h) Volla, C. M. R.; Das, A.; Atodiresei, I.; Rueping, M. *Chem. Commun.* **2014**, 7889–7892.
8. Kawasaki, M.; Yamamoto, H. *J. Am. Chem. Soc.* **2006**, 128, 16482–16483; Zhao, D.; Wu, Q.; Huang, X.; Song, F.; Lv, T.; You, J. *Chem.—Eur. J.* **2013**, 19, 6239–6244.
9. Jasiński, M.; Pocięcha, D.; Monobe, H.; Szczytko, J.; Kaszyński, P. *J. Am. Chem. Soc.* **2014**, 136, 14658–14661.
10. Mlostko, G.; Urbaniak, K.; Jacaszek, N.; Linden, A.; Heimgartner, H. *Heterocycles* **2014**, 88, 387–401.
11. Hansch, C.; Leo, A.; Taft, R. *Chem. Rev.* **1991**, 91, 165–195.
12. Bordwell, F. G. *Acc. Chem. Res.* **1988**, 21, 456–463.
13. Frisch, M. J.; Trucks, G. W.; Schlegel, H. B.; Scuseria, G. E.; Robb, M. A.; Cheeseman, J. R.; Scalmani, G.; Barone, V.; Mennucci, B.; Petersson, G. A.; Nakatsuji, H.; Caricato, M.; Li, X.; Hratchian, H. P.; Izmaylov, A. F.; Bloino, J.; Zheng, G.; Sonnenberg, J. L.; Hada, M.; Ehara, M.; Toyota, K.; Fukuda, R.; Hasegawa, J.; Ishida, M.; Nakajima, T.; Honda, Y.; Kitao, O.; Nakai, H.; Vreven, T.; Montgomery, J. A., Jr.; Peralta, J. E.; Ogliaro, F.; Bearpark, M.; Heyd, J. J.; Brothers, E.; Kudin, K. N.; Staroverov, V. N.; Kobayashi, R.; Normand, J.; Raghavachari, K.; Rendell, A.; Burant, J. C.; Iyengar, S. S.; Tomasi, J.; Cossi, M.; Rega, N.; Millam, J. M.; Klene, M.; Knox, J. E.; Cross, J. B.; Bakken, V.; Adamo, C.; Jaramillo, J.; Gomperts, R.; Stratmann, R. E.; Yazyev, O.; Austin, A. J.; Cammi, R.; Pomelli, C.; Ochterski, J. W.; Martin, R. L.; Morokuma, K.; Zakrzewski, V. G.; Voth, G. A.; Salvador, P.; Dannenberg, J. J.; Dapprich, S.; Daniels, A. D.; Farkas, O.; Foresman, J. B.; Ortiz, J. V.; Cioslowski, J.; Fox, D. *J. Gaussian 09, Revision A.02*; Gaussian: Wallingford, CT, 2009.
14. Zhao, Y.; Truhlar, D. G. *Theor. Chem. Acc.* **2008**, 120, 215–241.

15. Scott, A. P.; Radom, L. *J. Phys. Chem.* **1996**, *100*, 16502–16513.
16. Cossi, M.; Scalmani, G.; Rega, N.; Barone, V. *J. Chem. Phys.* **2002**, *117*, 43–54 and references therein.
17. Fulmer, G. R.; Miller, A. J. M.; Sherden, N. H.; Gottlieb, H. E.; Nudelman, A.; Stoltz, B. M.; Bercaw, J. E.; Goldberg, K. I. *Organometallics* **2010**, *29*, 2176–2179.
18. Stieber, F.; Grether, U.; Waldmann, H. *Chem.—Eur. J.* **2003**, *9*, 3270–3281.
19. Jasiński, M.; Gerding, J. S.; Jankowiak, A.; Gebicki, K.; Romański, J.; Jastrzębska, K.; Sivaramamorthy, A.; Mason, K.; Evans, D. H.; Celeda, M.; Kaszyński, P. *J. Org. Chem.* **2013**, *78*, 7445–7454.
20. Tanaka, K.; Maeno, S.; Mitsuhashi, K. *J. Heterocycl. Chem.* **1985**, *22*, 565–568.
21. Carroccia, L.; Fioravanti, S.; Pellacani, L.; Tardella, P. A. *Synthesis* **2010**, 4096–4100.